

Impacts of the intrinsic charm content of the proton on the Ξ_{cc} hadroproduction at a fixed target experiment at the LHC

Gu Chen^{1,*}, Xing-Gang Wu^{2,†} and Shuai Xu^{2,‡}

¹*School of Physics and Electronic Engineering, Guangzhou University, Guangzhou 510006, People's Republic of China*

²*Department of Physics, Chongqing University, Chongqing 401331, People's Republic of China*

(Dated: November 7, 2021)

In the present paper, we present detailed discussions on the hadronic production of Ξ_{cc} at a fixed target experiment at the LHC (After@LHC). The charm quarks in hadron could be either extrinsic or intrinsic. By using the BHPS model as the intrinsic charm distribution function in proton, we observe that even if by setting the proportion of finding the intrinsic charm in a proton as $A_{in} = 1\%$, total cross sections for the $g + c$ and $c + c$ production mechanisms shall be enhanced by nearly two times. Thus the number of Ξ_{cc} events to be generated at the After@LHC can be greatly enhanced. Since the total cross sections and differential distributions for the Ξ_{cc} production at the After@LHC are sensitive to the value of A_{in} , the After@LHC could be a good platform for testing the idea of intrinsic charm.

I. INTRODUCTION

Stimulating by the observation of the doubly charmed baryon Ξ_{cc}^{++} by the LHCb collaboration [1], people have shown many new interests on the doubly heavy baryons. More measurements are assumed to be done at the LHCb Upgrade II [2]. In the past decades, in addition to its decay properties, many theoretical works have been done for the production of the doubly heavy baryons at various high-energy colliders [3–29].

There are three important mechanisms for the production of Ξ_{cc} at the high-energy hadronic colliders such as LHC and Tevatron, which are through the gluon-gluon fusion ($g + g$), the gluon-charm collision ($g + c$), and the charm-charm collision ($c + c$), respectively. Those production mechanisms are pQCD calculable, since the intermediate gluon should be hard enough to generate a hard $c\bar{c}$ pair in the final state. For the ($g + c$) and ($c + c$) production mechanisms, one usually treats the incident charm quarks as “extrinsic” ones, which are perturbatively generated by gluon splitting according to the DGLAP evolution [30–32]. The hadronic production of Ξ_{cc} with “extrinsic” charm mechanism has been discussed in Refs. [33–35]. Those works show that the ($g + c$) mechanism dominates over the conventionally consider ($g + g$) fusion mechanism in small p_t region¹, and thus it is important for the fixed-target experiments such as the SELEX experiment at the Tevatron and the suggested fixed target experiment at the LHC (After@LHC) due to the measured Ξ_{cc} p_t could be very small [36–40].

In addition to the “extrinsic” ones, the incident c -quarks may also be “intrinsic” ones, which are correlated

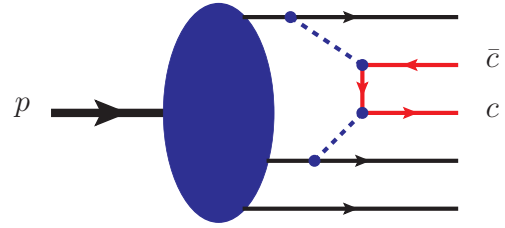


FIG. 1. Typical Feynman diagrams for the intrinsic mechanism through nonperturbative fluctuations of the proton state to five-quark Fock state. The dashed lines stand for soft interactions.

to the non-perturbative fluctuations of nucleon state to the five-quark state, as shown in Fig. 1. This idea has been proposed firstly by Brodsky *et al.*, and the BHPS model has been raised for estimating the intrinsic c -quark distribution in nucleon [41–43]. Lately, many more phenomenological studies have been done to illustrate the non-perturbative charm in nucleon, e.g., the meson-baryon model [44, 45], the sea-like model [46], and etc.. Because the proportion of the intrinsic charm components in nucleon is small, which is only up to $\sim 1\%$, the intrinsic charm usually gives negligible contribution in most of the high-energy processes. At present, due to lack of experimental measurements, definite conclusion on the existence of intrinsic charm is still missing.

It has been found that the Ξ_{cc} events generated at the SELEX are much more sensitive to the intrinsic charm than those at the hadronic colliders as LHC and the Tevatron [47–50]. There is hope to confirm the intrinsic components in proton by measuring the events in specific kinematic regions, such as small p_t region. The SELEX experiment has already been shut down and its puzzle on Ξ_{cc} observation, e.g., its measured production rate is much larger than most of the theoretical predictions [51, 52], remains unresolved. The intrinsic charm production mechanism may solve this puzzle [26]. And we still need more accurate fixed-target experimental

* email:speecgu@gzhu.edu.cn

† email:wuxg@cqu.edu.cn

‡ shuaixu@cqu.edu.cn

¹ In large p_t region, the cross section shall be highly suppressed by the charm quark distribution function; This explains why the gluon-gluon mechanism alone is usually adopted for analyzing the measurements with large p_t cut.

data to clarify the issue. At the LHC, when the incident proton beam energy rises up to 7 TeV, the proposed After@LHC will run with a center-of-mass energy around 115 GeV. With a much higher luminosity and higher collision energy, the After@LHC will become a much better fixed-target experiment for studying the properties of the doubly heavy baryons. It is thus interesting to investigate how and to what degree the intrinsic charm affects the Ξ_{cc} production at the After@LHC.

The remaining parts of the paper are organized as follows. In Sec.II, we present the calculation technology for the hadronic production of Ξ_{cc} . In Sec.III, we

present our numerical results and discussions for various Ξ_{cc} hadroproduction mechanisms, and show how the intrinsic charm affects the cross sections. Sec.IV is reserved for a summary.

II. CALCULATION TECHNOLOGY

Within the perturbative QCD factorization formula, the total cross section for the hadronic production of Ξ_{cc} can be factorized as follows,

$$\begin{aligned} \sigma(H_1 + H_2 \rightarrow \Xi_{cc} + X) = & \int dx_1 dx_2 \left\{ f_{H_1}^g(x_1, \mu) f_{H_2}^g(x_2, \mu) \otimes \hat{\sigma}_{g+g \rightarrow \Xi_{cc}}(x_1, x_2, \mu) \right. \\ & + \sum_{i,j=1,2; i \neq j} f_{H_i}^g(x_1, \mu) \left[f_{H_j}^c(x_2, \mu) - f_{H_j}^c(x_2, \mu)_{\text{SUB}} \right] \otimes \hat{\sigma}_{g+c \rightarrow \Xi_{cc}}(x_1, x_2, \mu) \\ & \left. + \sum_{i,j=1,2; i \neq j} f_{H_i}^c(x_1, \mu) f_{H_j}^c(x_2, \mu) \otimes \hat{\sigma}_{cc \rightarrow \Xi_{cc}}(x_1, x_2, \mu) + \dots \right\}, \end{aligned} \quad (1)$$

where we have implicitly set the factorization scale and renormalization scale to be the same, $\mu_F = \mu_R = \mu$. f_H^a ($a = (g, c)$) is parton distribution function (PDF) of the corresponding parton a in the incident hadron H . $f_H^c(x, \mu)_{\text{SUB}}$ is the subtraction term to avoid double counting problem between the $(g + g)$ and $(g + c)$ production mechanisms [53–56], which is defined as,

$$\begin{aligned} f_H^c(x, \mu)_{\text{SUB}} & \equiv f_H^g(x, \mu) \otimes f_g^c(x, \mu) \\ & = \int_x^1 \frac{dy}{y} f_g^c(y, \mu) f_H^g\left(\frac{x}{y}, \mu\right) \end{aligned} \quad (2)$$

with

$$\begin{aligned} f_g^c(x, \mu) & = \frac{\alpha_s(\mu)}{2\pi} \ln \frac{\mu^2}{m_c^2} P_{g \rightarrow q}(x) \\ & = \frac{\alpha_s(\mu)}{2\pi} \ln \frac{\mu^2}{m_c^2} \cdot \frac{1}{2} (1 - 2x + 2x^2). \end{aligned} \quad (3)$$

By taking the intrinsic charm component into account, the PDF f_H^a can be expressed as,

$$f_H^a(x, \mu) = f_H^{a,0}(x, \mu) + f_H^{a,\text{in}}(x, \mu), \quad (4)$$

where $f_H^{a,0}$ is the PDF without intrinsic charm effect, and $f_H^{a,\text{in}}(x, \mu)$ is the new term introduced by the intrinsic charm effect.

The PDF at any other scale can be obtained by applying the DGLAP equations with the known PDF $f_H^{a,\text{in}}(x, 2m_c)$ at the initial scale $2m_c$, i.e., [57]

$$\begin{aligned} f_H^{c,\text{in}}(x, \mu) = & \int_x^1 \frac{dy}{y} \left\{ f_H^{c,\text{in}}(x/y, 2m_c) \frac{[-\ln(y)]^{a_c \kappa - 1}}{\Gamma(a_c \kappa)} \right\} + \\ & \kappa \int_x^1 \frac{dy}{y} \int_y^1 \frac{dz}{z} \left\{ f_H^{c,\text{in}}(y/z, 2m_c) \frac{[-\ln(z)]^{a_c \kappa - 1}}{\Gamma(a_c \kappa)} P_{\Delta c}(x/y) \right\} + \mathcal{O}(\kappa^2), \end{aligned} \quad (5)$$

$$f_H^{g,\text{in}}(x, \mu) = \frac{2\kappa}{a_g - a_c} \int_x^1 \frac{dy}{y} \int_{a_c}^{a_g} da \int_y^1 \frac{dz}{z} \left\{ f_H^{c,\text{in}}(z, 2m_c) \frac{[-\ln(z)]^{a\kappa - 1}}{\Gamma(a\kappa)} P_{c \rightarrow gc}(x/y) \right\} + \mathcal{O}(\kappa^2), \quad (6)$$

with

$$a_g = 6, \quad a_c = \frac{8}{3}, \quad \beta_0 = 11 - 2n_f/3,$$

$$\kappa = \frac{2}{\beta_0} \ln \left(\frac{\alpha_s(2m_c)}{\alpha_s(\mu)} \right),$$

$$P_{\Delta c}(x) = \frac{4}{3} \left[\frac{1+x^2}{1-x} + \frac{2}{\ln x} + \left(\frac{3}{2} - 2\gamma_E \right) \delta(1-x) \right],$$

$$P_{c \rightarrow gc} = \frac{4}{3} \left[\frac{1+(1-x)^2}{x} \right]. \quad (7)$$

In doing the numerical analysis, we adopt the BHPS model [41] for the PDF $f_H^{c,\text{in}}(x, 2m_c)$ as a typical one to discuss the intrinsic charm's effect, e.g.,

$$f_H^{c,\text{in}}(x, 2m_c) = 6x^2\xi \left[6x(1+x)\ln x + (1-x)(1+10x+x^2) \right], \quad (8)$$

where the parameter ξ is fixed by the probability of finding the intrinsic charm quark, which satisfies the normalization condition as,

$$A_{\text{in}} \equiv \int_0^1 f_H^{c,\text{in}}(x, 2m_c) dx = \xi \times 1\%.$$

The probability for finding intrinsic c/\bar{c} -component in proton at the fixed low-energy scale $2m_c$ is assumed to be less than 1% [41, 42], and we set a broader range of $\xi \in [0.1, 1]$ to do the discussion.

Many effects have been paid to the intrinsic charm (IC) PDF [58–65], which are usually fixed via global fitting of experimental data. For example, the CTEQ group, firstly suggested the CTEQ6.5C PDF version [58] by carrying out a series of global fits with varying magnitudes of IC components. That is, the intrinsic charm component is characterized by the first moment of the c -quark and \bar{c} -antiquark momentum distributions,

$$\langle x \rangle_{c+\bar{c}} = \int_0^1 x [c(x) + \bar{c}(x)] dx, \quad (9)$$

where the distributions $c(x)$ and $\bar{c}(x)$ depend on the IC models such as the BHPS model (8), the Meson-Cloud Model (MCM) with the IC arises from virtual low-mass

meson+baryon components, e.g., $\bar{D}^0\Lambda_c^+$, in a proton, and the sea-like model with IC is assumed to behave as the light flavor sea quarks, e.g. $c(x) = \bar{c}(x)$ is proportional to $\bar{d}(x) + \bar{u}(x)$ with an overall charm mass suppression. Lately, the CTEQ group improved it as CTEQ6.6C [59] IC PDF version by taking both the BHPS and the sea-like models into account with moderate and large IC contributions as 1% and 3.5% (corresponding to $\langle x \rangle_{c+\bar{c}} = 0.57\%$ and 2%, respectively), which then improved as CT10C [61] and CT14C [65] by taking more data into consideration. As another example, the MSTW group issued the MSTW2008 IC PDF version [60] by dealing with the IC component under the general-mass variable flavour number scheme. And recently the NNPDF group developed a model independent NNPDF3IC IC version [64], whose input parameters are based on a NLO calculation and are fixed via a global fitting of experimental data of deep inelastic structure functions.

III. NUMERICAL RESULTS AND DISCUSSIONS

The doubly charmed baryon Ξ_{cc} can be produced by first perturbatively forming a (cc) pair via $g + g \rightarrow (cc) + \bar{c}\bar{c}$, $g + c \rightarrow (cc) + \bar{c}$ or $c + c \rightarrow (cc) + g$ channels, then forming a bound (cc) -diquark state either in spin-triplet and color anti-triplet state $(cc)_{\bar{3}}[{}^3S_1]$ or in spin-singlet and color sextuplet state $(cc)_{\mathbf{6}}[{}^1S_0]$, and finally, hadronizing into the Ξ_{cc} baryon. To be the same as those of Ref.[34], we take the probability for a (cc) -pair to transform into the Ξ_{cc} -baryon as $|\Psi_{cc}(0)|^2 = 0.039 \text{ GeV}^3$, $M_{\Xi_{cc}} = 3.50 \text{ GeV}$ with $m_c = M_{\Xi_{cc}}/2$. We take the CT14LO PDF version [66], which is issued by the CTEQ group, as the input for the PDF $f_H^{a,0}(x, \mu)$ without intrinsic charm effect.

-	σ_{g+g} (pb)		σ_{g+c} (pb)		σ_{c+c} (pb)	
	$(cc)_{\bar{3}}[{}^3S_1]$	$(cc)_{\mathbf{6}}[{}^1S_0]$	$(cc)_{\bar{3}}[{}^3S_1]$	$(cc)_{\mathbf{6}}[{}^1S_0]$	$(cc)_{\bar{3}}[{}^3S_1]$	$(cc)_{\mathbf{6}}[{}^1S_0]$
$A_{\text{in}} = 0$	7.44×10^2	1.35×10^2	3.07×10^3	3.34×10^2	1.02	4.12×10^{-2}
$A_{\text{in}} = 0.1\%$	7.47×10^2	1.35×10^2	3.31×10^3	3.59×10^2	1.09	4.38×10^{-2}
$A_{\text{in}} = 0.3\%$	7.49×10^2	1.36×10^2	3.76×10^3	4.07×10^2	1.24	4.98×10^{-2}
$A_{\text{in}} = 1\%$	7.55×10^2	1.37×10^2	5.32×10^3	5.78×10^2	1.79	7.16×10^{-2}

TABLE I. Total cross sections of the Ξ_{cc} production at the After@LHC with different intrinsic charm component corresponding to different choices of A_{in} , which are 0, 0.1%, 0.3%, and 1%, respectively. $A_{\text{in}} = 0$ means no intrinsic charm component has been taken into consideration. $p_t > 0.2 \text{ GeV}$.

In the literature, a generator GENXICC [67–69] has been programmed, which can be conveniently used for

simulating the Ξ_{cc} events at the hadronic colliders. Our numerical calculations shall be done by using the gen-

erator GENXICC with proper changes to include both the extrinsic and intrinsic charm effects in the charm and gluon PDFs. The probability of finding the intrinsic charm in proton is set as $A_{\text{in}} = 0, 0.1\%, 0.3\%$, and 1% , respectively, where $A_{\text{in}} = 0$ corresponds to the extrinsic mechanism. We have implicitly taken a small transverse momentum (p_t) cut for the Ξ_{cc} events, i.e., $p_t > 0.2$ GeV, which is the same as the SELEX and could also be adopted by the fixed-target experiment After@LHC.

As an overall impression, we present the total cross sections for the Ξ_{cc} production at the After@LHC via the $(g + g)$, $(g + c)$, and $(c + c)$ production mechanisms in Table I, where the results for $(cc)_{\bar{3}}[{}^3S_1]$ and $(cc)_{\bar{6}}[{}^1S_0]$ are presented. Table I shows that for each production channels, the intermediate $(cc)_{\bar{6}}[{}^1S_0]$ can also give sizable contributions, e.g. its production cross sections for $(g + g)$, $(g + c)$, and $(c + c)$ production mechanisms are about 18%, 11% and 4% of the corresponding $(cc)_{\bar{3}}[{}^3S_1]$ cross sections. Table I also shows how the total cross sections vary with the increment of intrinsic charm components in proton, which shall give sizable contributions to the $(g + c)$ and $(c + c)$ mechanisms. For example, even if there is only one-in-one-thousand probability to find the intrinsic charm component in proton, e.g. $A = 0.1\%$, the total cross sections for $(g + c)$ and $(c + c)$ mechanisms shall be increased by about 7%.

A. Ξ_{cc} production via the $(g + g)$ fusion mechanism

-	$p_t \geq 2$ GeV	$p_t \geq 4$ GeV	$p_t \geq 6$ GeV	$p_t \geq 8$ GeV
$\sigma_{g+g}^{(cc)_{\bar{3}}[{}^3S_1]}$	2.71×10^2	3.21×10^1	3.59	4.81×10^{-1}
$\sigma_{g+g}^{(cc)_{\bar{6}}[{}^1S_0]}$	5.85×10^1	9.06	1.21	1.80×10^{-1}

TABLE II. Total cross sections (in unit pb) for the Ξ_{cc} production via $(g + g)$ channel at the After@LHC under different p_t cuts, where we have set $A_{\text{in}} = 1\%$.

-	$ y < 1$	$ y < 2$	$ y < 3$
$\sigma_{g+g}^{(cc)_{\bar{3}}[{}^3S_1]}$	4.97×10^2	7.28×10^2	7.57×10^2
$\sigma_{g+g}^{(cc)_{\bar{6}}[{}^1S_0]}$	8.92×10^1	1.32×10^2	1.37×10^2

TABLE III. Total cross sections (in unit pb) for the Ξ_{cc} production via $(g + g)$ channel at the After@LHC under different y cuts, where we have set $A_{\text{in}} = 1\%$ and $p_t > 0.2$ GeV.

As for $(g + g)$ fusion mechanism, total cross sections with intrinsic charm $A_{\text{in}} = 1\%$ under various kinematic cuts are presented in Tables II and III. It's found that the impacts of intrinsic charm on the $(g + g)$ channel is less than 2% even by setting $A_{\text{in}} = 1\%$. There are nearly 96% Ξ_{cc} events to be generated in small p_t region, $p_t \in [0, 4$ GeV], and about 66% Ξ_{cc} events for $|y| \leq 1$. Thus for a fixed-target experiment as After@LHC, in which small p_t events can be detected, a more accurate production information on Ξ_{cc} can be achieved.

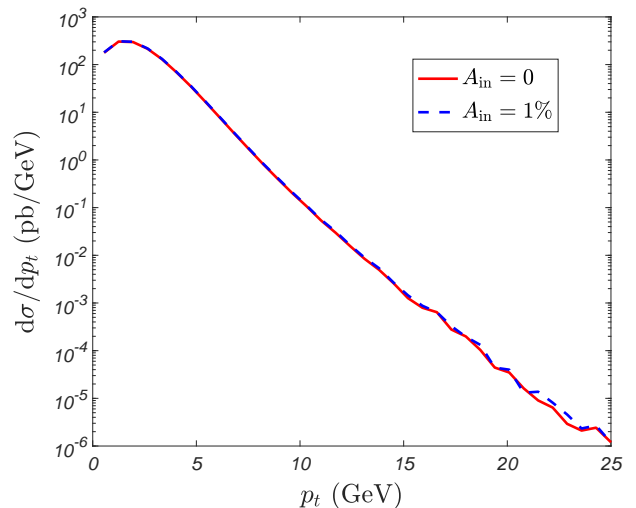


FIG. 2. Comparison of the p_t distributions for the hadroproduction of Ξ_{cc} with and without intrinsic charm, $A_{\text{in}} = 1\%$ and $A_{\text{in}} = 0$, via the $g + g$ production mechanism at the After@LHC. Here contributions from various intermediate diquark states have been summed up.

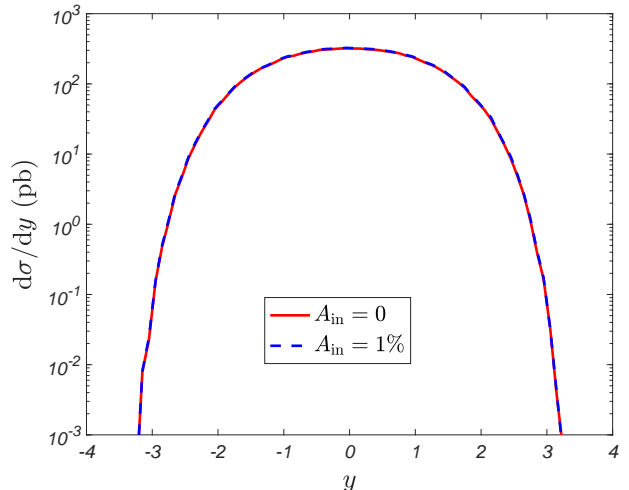


FIG. 3. Comparison of the y distributions for the hadroproduction of Ξ_{cc} with and without intrinsic charm, $A_{\text{in}} = 1\%$ and $A_{\text{in}} = 0$, via the $g + g$ production mechanism at the After@LHC. Here contributions from various intermediate diquark states have been summed up. $p_t > 0.2$ GeV.

For the differential productions of Ξ_{cc} , we investigate the differential distributions with respect to the p_t and y as presented in Figs. 2 and 3, respectively. Both the cases with and without intrinsic charm are plotted, in which the contributions from $(cc)_{\bar{3}}[{}^3S_1]$ and $(cc)_{\bar{6}}[{}^1S_0]$ diquark states have summed up. In those figures, the solid and the dashed lines stand for the differential distributions without and with intrinsic charm, which correspond to $A_{\text{in}} = 0$ and $A_{\text{in}} = 1\%$, respectively. Fig. 2 shows that the p_t -distribution drops quickly with the increment of p_t .

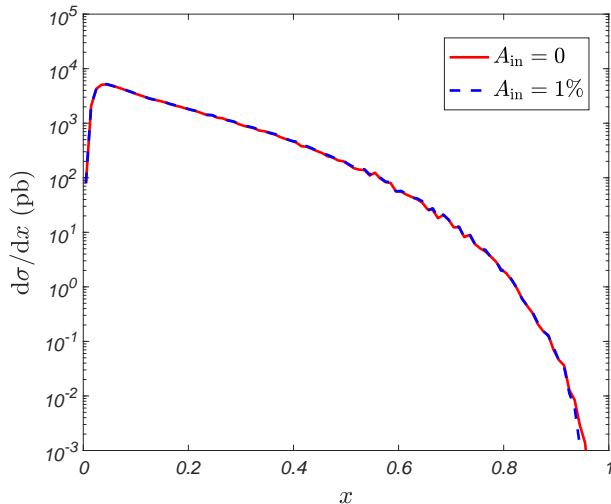


FIG. 4. Comparison of the x distributions for the hadroproduction of Ξ_{cc} with and without intrinsic charm, $A_{in} = 1\%$ and $A_{in} = 0$, via the $g + g$ production mechanism at the After@LHC. Here contributions from various intermediate diquark states have been summed up. $p_t > 0.2$ GeV.

Fig.3 shows that there is a small plateau within $|y| \leq 1.5$ for the Ξ_{cc} production via the $(g + g)$ channel. In Fig. 4, we plot the x distributions of Ξ_{cc} production with and without intrinsic charm via the $(g + g)$ scheme.

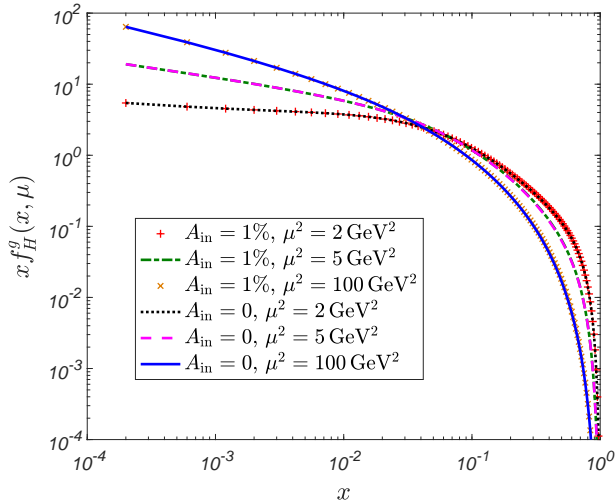


FIG. 5. The gluon PDF with and without intrinsic charm, $A_{in} = 1\%$ and $A_{in} = 0$, at different scales (μ^2).

Figs. 2 and 3 indicate that the p_t and y shapes of Ξ_{cc} change very slightly in whole p_t or y region by taking the intrinsic charm component into consideration. This is due to the fact that the impacts of intrinsic charm to the gluon PDF, as expressed by Eq. (6), is small. We present a comparison of the gluon PDF with and without intrinsic charm effects in Fig. 5, where three typical

scales, $\mu^2 = 2$ GeV², 5 GeV², 100 GeV², are adopted. The nearly coincidence of the two curves with and without intrinsic charm under various scales, indicating the effect of intrinsic charm to the gluon PDF is negligible.

B. Ξ_{cc} production via $(g + c)$ and $(c + c)$ channels with extrinsic charm mechanism

In addition to the $(g + g)$ channel, the gluon-charm $(g + c)$ and the charm-charm $(c + c)$ interactions are important for a sound prediction of the Ξ_{cc} hadronic production. In this subsection, we study the hadronic production properties of Ξ_{cc} via the $(g + c)$ and $(c + c)$ channel at the After@LHC experiment, where the c quark is extrinsic one only.

To see more explicitly how these channels affect the Ξ_{cc} production cross sections, we define a ratio \mathcal{R} based on the cross section of the frequently considered channel $g + g \rightarrow \Xi_{cc}(cc)\bar{3}[{}^3S_1] + \bar{c} + \bar{c}$, i.e.,

$$\mathcal{R} = \frac{\sigma_{\text{tot}}}{\sigma_{g+g \rightarrow \Xi_{cc}(cc)\bar{3}[{}^3S_1]}}, \quad (10)$$

where σ_{tot} stands for the total cross sections of all the concerned production mechanisms and intermediate diquark states. The values of \mathcal{R} shall be shown in Table IV, where $A_{in} = 0$ indicates the extrinsic charm components, whose contribution is large in comparison to the $(g + g)$ -mechanism, e.g., $\mathcal{R} = 5.8$ for $A_{in} = 0$.

In Table I, the results for $A_{in} = 0$ are cross sections for extrinsic charm mechanisms. For the $(g + c)$ channel, total cross sections from the diquark state $(cc)\bar{3}[{}^3S_1]$ are about 9 times bigger than those from $(cc)\bar{6}[{}^1S_0]$. For the $(c + c)$ channel, total cross sections from the diquark state $(cc)\bar{3}[{}^3S_1]$ are about 10 times bigger than those from $(cc)\bar{6}[{}^1S_0]$. By summing up different diquark contributions, the relative importance of the cross sections among different production channels is

$$\sigma_{g+g}^{A_{in}=0} : \sigma_{g+c}^{A_{in}=0} : \sigma_{c+c}^{A_{in}=0} \simeq 8.3 \times 10^2 : 3.2 \times 10^3 : 1.$$

We observe that the cross section for the $(g + c)$ -channel is dominant over that of $(c + c)$ -channel by about three orders, which is about four times of the cross section of the $(g + g)$ -channel. This confirms the necessity for including the charm-initiated channels in the calculations.

C. The intrinsic charm effects in Ξ_{cc} production via $(g + c)$ and $(c + c)$ channels

In this subsection we show how the total production cross sections are altered by further taking into account the intrinsic charm.

By varying the intrinsic component A_{in} from 0.1% to 1%, the cross sections of $(g + c)$ and $(c + c)$ channels have been presented in Table I. The cross sections of $(g + c)$ and $(c + c)$ channels are enhanced by about 7.5% to 75%

with increment of the intrinsic charm component $A_{\text{in}} \in [0.1\%, 1\%]$. More explicitly, if taking the intrinsic charm component as $A_{\text{in}} = 1\%$, the relative importance of cross sections among different channels is

$$\sigma_{g+g}^{A_{\text{in}}=1\%} : \sigma_{g+c}^{A_{\text{in}}=1\%} : \sigma_{c+c}^{A_{\text{in}}=1\%} \simeq 4.8 \times 10^2 : 3.2 \times 10^3 : 1.$$

Comparing with the extrinsic case, we find that the relative importance of $(g+c)$ and $(c+c)$ channels are enhanced by taking the intrinsic charm into consideration.

	$A_{\text{in}} = 0$	$A_{\text{in}} = 0.1\%$	$A_{\text{in}} = 0.3\%$	$A_{\text{in}} = 1\%$
\mathcal{R}	5.8	6.1	6.7	9.0

TABLE IV. The \mathcal{R} values defined in Eq. (10) at the After@LHC with various choices of A_{in} . $A_{\text{in}} = 0$ indicates that only the extrinsic mechanisms are considered. $p_t > 0.2$ GeV.

We present the \mathcal{R} ratios under different choices of intrinsic charm components in Table IV. Table IV shows the production cross section under extrinsic mechanisms shall be highly affected by the intrinsic charm, e.g., when $A_{\text{in}} = 1\%$, the \mathcal{R} ratio shall be increased by 55%.

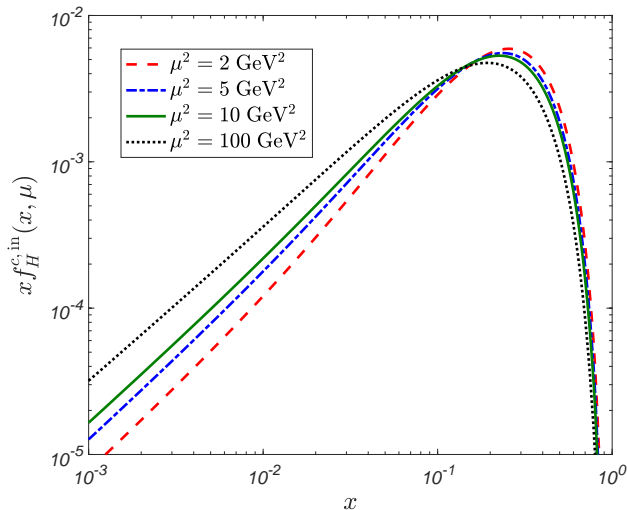


FIG. 6. Scale evolution of the intrinsic charm PDF defined in Eq. (5). $A_{\text{in}} = 1\%$.

To account for these points, we illustrate how the intrinsic charm component affects the charm PDF. First, we present the x -distribution of intrinsic charm with $A_{\text{in}} = 1\%$ under several typical scales in Fig. 6. Fig. 6 shows the intrinsic charm PDF increases in small x region and decreases in high x , whose peak slightly moves with varying scales. Second, we present the total charm PDF, defined in Eq. (4), with various intrinsic charm components in Fig. 7. It shows the total charm PDF has a small humped behavior around $x \sim 0.3$. This peaked behavior explains the strong enhancement of the intrinsic charm to the Ξ_{cc} production via $(g+c)$ and $(c+c)$ channels

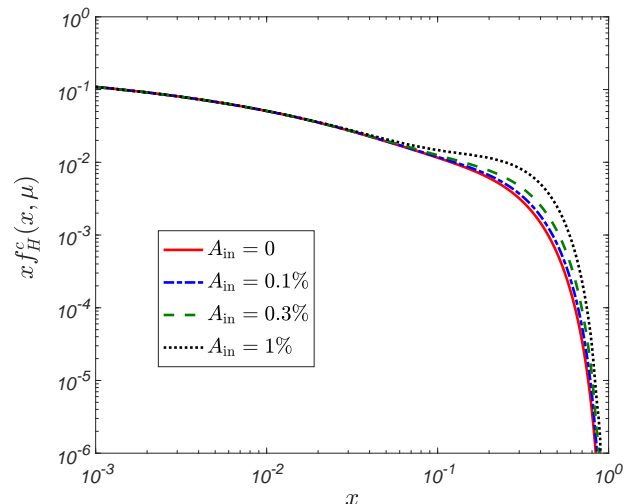


FIG. 7. Total charm PDF defined in Eq. (4) with various intrinsic charm components characterized by $A_{\text{in}} = 0 \sim 1\%$. $\mu^2 = 5$ GeV².

at the After@LHC. Thus, the intrinsic charm, if exists in hadrons, shall play an important role in the hadronic production of Ξ_{cc} .

Summing up the contributions from different intermediate diquark states and various production channels together, we obtain $\sigma_{\text{tot}}^{A_{\text{in}}=0} = 4.28 \times 10^3$ pb and $\sigma_{\text{tot}}^{A_{\text{in}}=1\%} = 6.79 \times 10^3$ pb. If the integrated luminosity at the After@LHC reaches 0.05 fb^{-1} or 2 fb^{-1} per operation year [36], the Ξ_{cc} events to be generated at the After@LHC shall be about 2.1×10^5 or 8.6×10^6 per operation year for $A_{\text{in}} = 0$. If setting $A_{\text{in}} = 1\%$, the Ξ_{cc} events shall be greatly increased to 3.4×10^5 or 1.4×10^7 per operation year. Thus to compare with the hadronic production at the LHC which usually adopts a larger p_t cut, the fixed-target experiment After@LHC could provide a better platform for studying the Ξ_{cc} properties and for testing the existence of intrinsic charm.

	$p_t \geq 2$ GeV	$p_t \geq 4$ GeV	$p_t \geq 6$ GeV	$p_t \geq 8$ GeV
$\sigma_{g+c}^{(cc)\bar{3}[^3S_1]}$	1.26×10^3	8.93×10^1	8.75	1.18
$\sigma_{g+c}^{(cc)\bar{6}[^1S_0]}$	1.47×10^2	1.52×10^1	1.78	2.73×10^{-1}
σ_{g+c}^0	8.04×10^2	5.81×10^1	5.56	7.48×10^{-1}
$\sigma_{c+c}^{(cc)\bar{3}[^3S_1]}$	1.79	1.79	1.54	3.38×10^{-1}
$\sigma_{c+c}^{(cc)\bar{6}[^1S_0]}$	7.16×10^{-2}	7.16×10^{-2}	5.89×10^{-2}	1.05×10^{-2}
σ_{c+c}^0	1.06	1.06	8.96×10^{-1}	1.70×10^{-1}

TABLE V. Total cross sections (in unit pb) for the Ξ_{cc} production at the After@LHC under different p_t cuts, where we have set $A_{\text{in}} = 1\%$. The total cross sections for $A_{\text{in}} = 0$ are presented as a comparison, e.g., σ^0 stands for the Ξ_{cc} production without intrinsic charm, where contributions of different diquark configuration have been summed up.

For convenience of comparing with the future experi-

	$ y < 1$	$ y < 2$	$ y < 3$
$\sigma_{g+c}^{(cc)\bar{3}[^3S_1]}$	2.28×10^3	4.50×10^3	5.27×10^3
$\sigma_{g+c}^{(cc)\bar{6}[^1S_0]}$	2.54×10^2	4.94×10^2	5.78×10^2
σ_{gc}^0	1.98×10^3	3.16×10^3	3.39×10^3
$\sigma_{c+c}^{(cc)\bar{3}[^3S_1]}$	1.43	1.79	1.79
$\sigma_{c+c}^{(cc)\bar{6}[^1S_0]}$	5.66×10^{-2}	7.14×10^{-2}	7.16×10^{-2}
σ_{cc}^0	8.92×10^{-1}	1.06	1.06

TABLE VI. Total cross sections (in unit pb) for the Ξ_{cc} production at the After@LHC under different y cuts, where we have set $A_{\text{in}} = 1\%$. The total cross sections for $A_{\text{in}} = 0$ are presented as a comparison, e.g., σ^0 stands for the Ξ_{cc} production without intrinsic charm, where contributions of different diquark configuration have been summed up. $p_t > 0.2$ GeV.

mental measurements, we present total cross sections under various kinematic cuts in Tables V and VI, where we have set $A_{\text{in}} = 1\%$. Tables V shows the results for typical transverse momentum cuts, $p_t \geq 2$ GeV, $p_t \geq 4$ GeV, $p_t \geq 6$ GeV, and $p_t \geq 8$ GeV, respectively. There are over 98% contributions are concentrated in small p_t region $[0, 4\text{GeV}]$. Table VI shows the results under three rapidity cuts, $|y| \leq 1$, $|y| \leq 2$, and $|y| \leq 3$.

	$p_t \geq 2$ GeV	$p_t \geq 4$ GeV	$p_t \geq 6$ GeV	$p_t \geq 8$ GeV
$\varepsilon_{g+c}(p_{t\text{cut}})$	75%	80%	89%	94%
$\varepsilon_{c+c}(p_{t\text{cut}})$	75%	75%	78%	105%

TABLE VII. The values of $\varepsilon_i(p_{t\text{cut}})$ defined in Eq. (11) for the hadronic production of Ξ_{cc} at the After@LHC with $A_{\text{in}} = 1\%$.

y_{cut}	$ y \leq 1$	$ y \leq 2$	$ y \leq 3$
$\zeta_{g+c}(y_{\text{cut}})$	28%	58%	73%
$\zeta_{c+c}(y_{\text{cut}})$	67%	76%	76%

TABLE VIII. The values of $\zeta_i(y_{\text{cut}})$ defined in Eq. (12) for the hadronic production of Ξ_{cc} at the After@LHC with $A_{\text{in}} = 1\%$. $p_t > 0.2$ GeV.

To see how the kinematic cuts affect the intrinsic charm contributions, we introduce two variables $\varepsilon_i(p_{t\text{cut}})$ and $\zeta_i(y_{\text{cut}})$:

$$\varepsilon_i(p_{t\text{cut}}) = \frac{\sigma_i(p_t \geq p_{t\text{cut}}) - \sigma_i^0(p_t \geq p_{t\text{cut}})}{\sigma_i^0(p_t \geq p_{t\text{cut}})} \times 100\% \quad (11)$$

and

$$\zeta_i(y_{\text{cut}}) = \frac{\sigma_i(|y| \leq y_{\text{cut}}) - \sigma_i^0(|y| \leq y_{\text{cut}})}{\sigma_i^0(|y| \leq y_{\text{cut}})} \times 100\% \quad (12)$$

where $i = g + c$ or $i = c + c$ stands for the contribution from the production channel $g + c \rightarrow \Xi_{cc}$ or $c + c \rightarrow \Xi_{cc}$, respectively. σ_i^0 is the cross section without intrinsic

charm and σ_i denotes that with $A_{\text{in}} = 1\%$, in which contributions of different diquark configuration have been summed up. The values of ε_i and ζ_i with different p_t cuts and y cuts are given in Tables VII and VIII. From Table VII, one can see that the relative importance of the intrinsic charm increases with increment of p_t cuts, e.g., ε_{g+c} varies from 75% to 94% and ε_{c+c} varies from 75% to 105% by taking the p_t cut from 2 GeV to 8 GeV. As shown in Table VIII, the ratio of intrinsic charm contributions ζ_i significantly increase from 28% to 73% for the $(g + c)$ channel and mildly increase from 67% to 73% for the $(c + c)$ channel with the increment of y_{cut} .

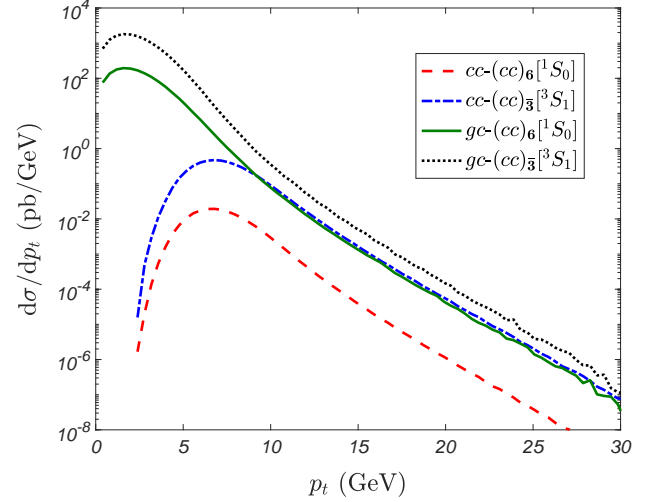


FIG. 8. The p_t distributions of Ξ_{cc} for various intermediate diquark states at the After@LHC with intrinsic charm component as $A_{\text{in}} = 1\%$, in which no y cut has been applied.

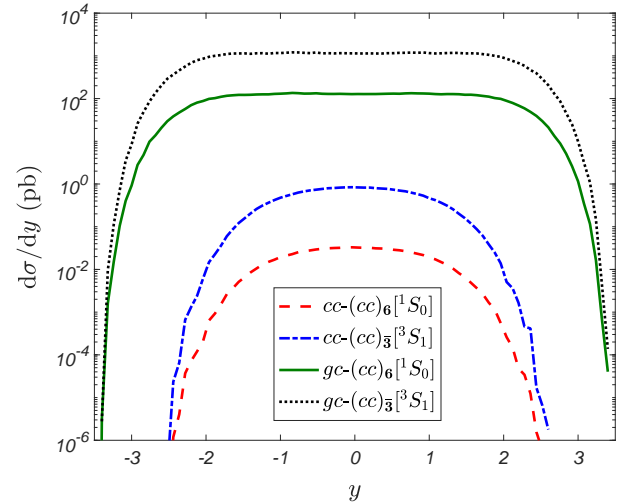


FIG. 9. The y distributions of Ξ_{cc} for various intermediate diquark states at the After@LHC with intrinsic charm component as $A_{\text{in}} = 1\%$. $p_t > 0.2$ GeV.

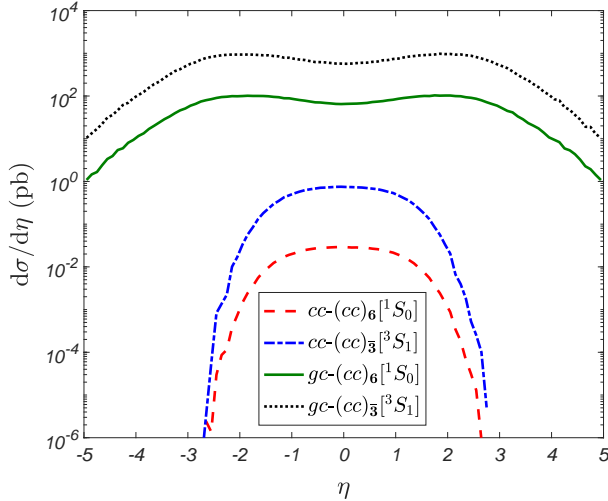


FIG. 10. The η distributions of Ξ_{cc} for various intermediate diquark states at the After@LHC with intrinsic charm component as $A_{\text{in}} = 1\%$. $p_t > 0.2$ GeV.

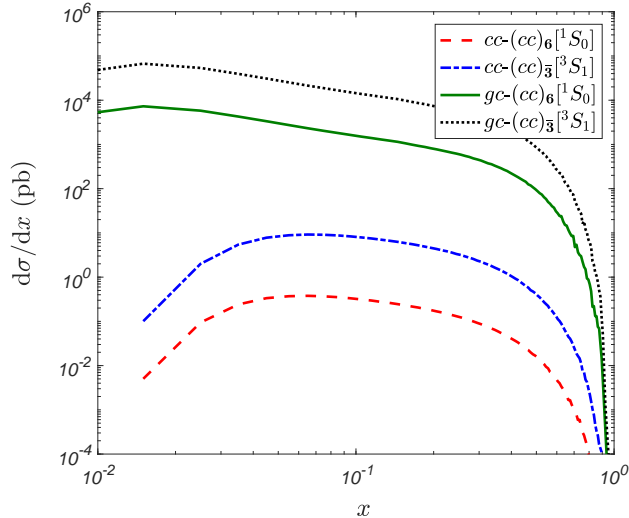


FIG. 11. The x distributions of Ξ_{cc} for various intermediate diquark states at the After@LHC with intrinsic charm component as $A_{\text{in}} = 1\%$. $p_t > 0.2$ GeV.

We present the Ξ_{cc} distributions at the After@LHC versus the transverse momentum (p_t), rapidity (y), and pseudo-rapidity (η) in Figs. 8, 9, and 10, respectively. Those distributions are consistent with the results in Tables VII and VIII. To compare with Fig. 2, Fig. 8 shows the Ξ_{cc} production in small p_t region is dominated by the $(g+c)$ channel, and the $(g+g)$ channel still dominates over the $(c+c)$ channel in almost the whole p_t region. Figs. 9 and 10 show the plateaus of $|y| \leq 1.5$ and $|\eta| \leq 2$ appear in $c+c$ channel, which become broader in $g+c$ channel as $|y| \leq 3$ and $|\eta| \leq 3$. We plot x distribution for the Ξ_{cc} production in the $(g+c)$ and $(c+c)$ subprocesses as shown in Fig. 11. Contributions from small x

range play the dominant role in the Ξ_{cc} production both in $(g+c)$ and $(c+c)$ channels.

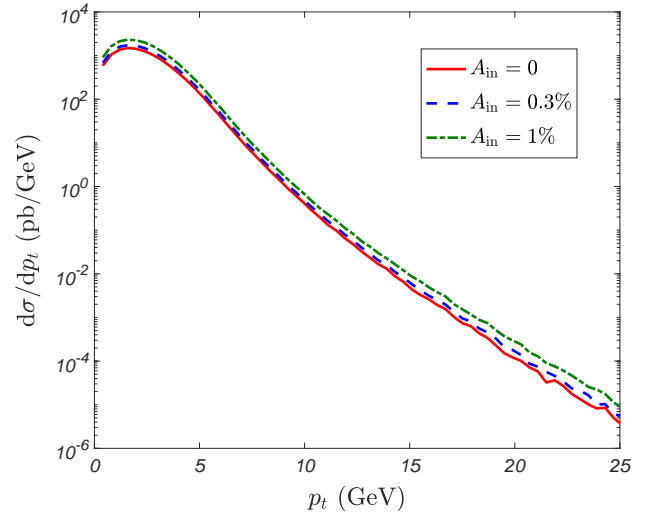


FIG. 12. The comparison of p_t distributions for the hadroproduction of Ξ_{cc} under different choices of A_{in} at the After@LHC, where contributions from various production schemes, i.e., $(g+g)$, $(g+c)$, and $(c+c)$, have been summed up. $p_t > 0.2$ GeV and no y cut has been applied.

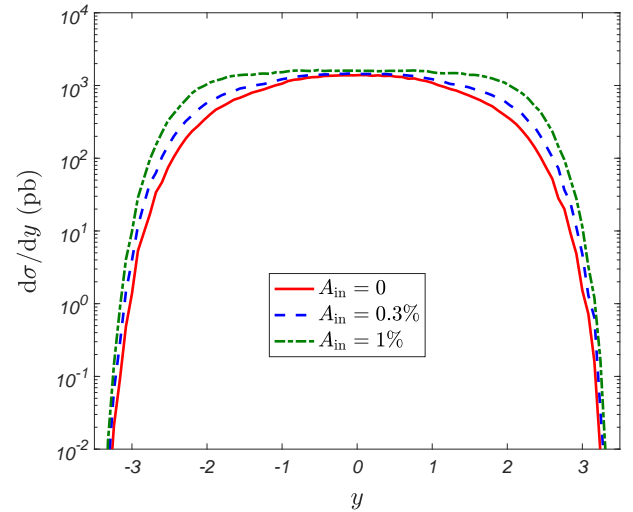


FIG. 13. The comparison of y distributions for the hadroproduction of Ξ_{cc} under different choices of A_{in} at the After@LHC, where contributions from various production schemes, i.e., $(g+g)$, $(g+c)$, and $(c+c)$, have been summed up. $p_t > 0.2$ GeV and no y cut has been applied.

To show how the intrinsic charm affects the differential distributions, we present the p_t , y , η , and x distributions for $A_{\text{in}} = 0, 0.3\%, 1\%$ in Figs. 12, 13, and 14, respectively. Here the contributions of $(cc)_{\bar{3}}[{}^3S_1]$ and $(cc)_{\bar{6}}[{}^1S_0]$ configurations, and results from different production schemes, i.e., $(g+g)$, $(g+c)$, and $(c+c)$, have

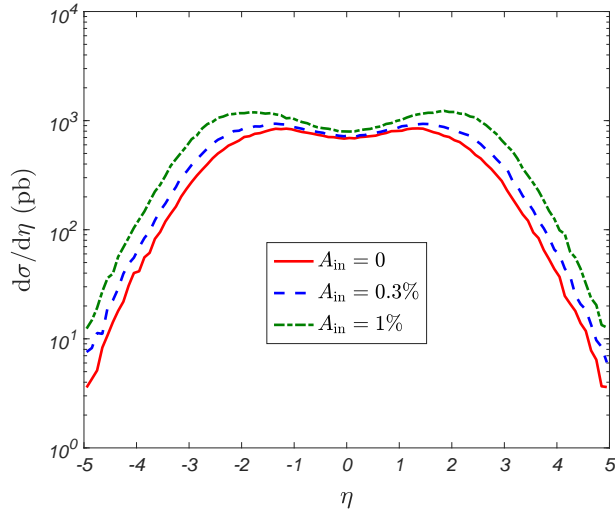


FIG. 14. The comparison of η distributions for the hadroproduction of Ξ_{cc} under different choices of A_{in} at the After@LHC, where contributions from various production schemes, i.e., $(g+g)$, $(g+c)$, and $(c+c)$, have been summed up. $p_t > 0.2$ GeV and no y cut has been applied.

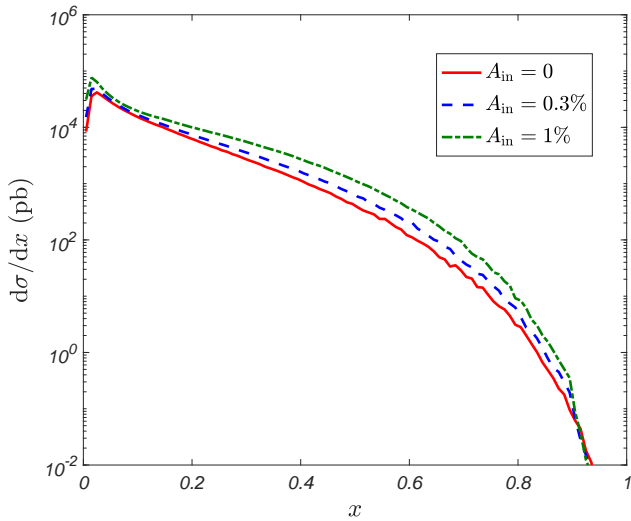


FIG. 15. The comparison of x distributions for the hadroproduction of Ξ_{cc} under different choices of A_{in} at the After@LHC, where contributions from various production schemes, i.e., $(g+g)$, $(g+c)$, and $(c+c)$, have been summed up. $p_t > 0.2$ GeV and no y cut has been applied.

been summed up. The p_t distributions are close in shape for various A_{in} , however their differences become obvious in large p_t region. The y and η distributions change more significantly with variation of A_{in} from 0 to 1%. For example, both the shape and the normalization of y -distribution are changed significantly with the increment of A_{in} . In Fig. 15, we present the comparison of x distributions with different intrinsic charm component. It shows that the intrinsic charm provides contribution

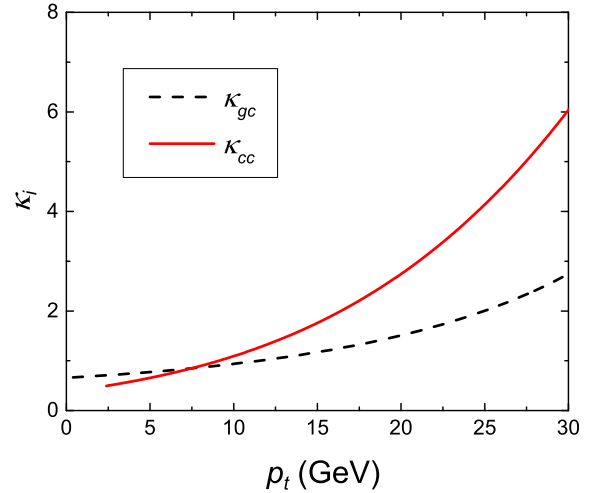


FIG. 16. The κ_i ($i = g+c, c+c$) defined in Eq. (13) versus p_t of Ξ_{cc} with intrinsic charm component $A_{\text{in}} = 1\%$ at the After@LHC, in which contributions from different intermediate diquark states have been summed up. $p_t > 0.2$ GeV and no y cut are applied.

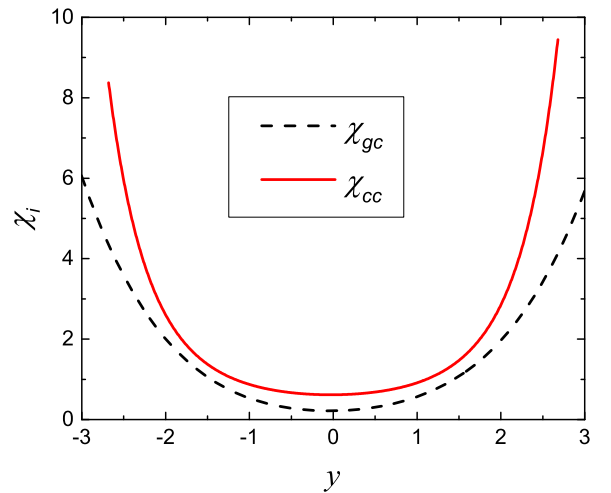


FIG. 17. The χ_i ($i = g+c, c+c$) defined in Eq. (14) versus y of Ξ_{cc} with intrinsic charm component $A_{\text{in}} = 1\%$ at the After@LHC, in which contributions from different intermediate diquark states have been summed up. $p_t > 0.2$ GeV and no y cut are applied.

in large x region, which is consistent with previous results as shown in Fig. 7. These changes of distributions are large enough to be potentially observed by the After@LHC for searching the intrinsic charm component in a proton. To show how the distributions change with the transverse momentum and rapidity, similar to the ratios $\varepsilon_i(p_{t\text{cut}})$ and $\zeta_i(y_{\text{cut}})$, we introduce two ratios κ_i and χ_i ,

i.e.?

$$\kappa_i = \frac{d\sigma_i/dp_t - d\sigma_i^0/dp_t}{d\sigma_i^0/dp_t}, \quad (13)$$

and

$$\chi_i = \frac{d\sigma_i/dy - d\sigma_i^0/dy}{d\sigma_i^0/dy}. \quad (14)$$

Here subscript i stands for $g + c$ or $c + c$ mechanism, respectively. σ denotes the cross section of $A_{\text{in}} = 1\%$ and σ^0 denotes that of $A_{\text{in}} = 0$, in which contributions of different diquark configuration have been summed up. The results are put in Figs. 16 and 17, which show in larger p_t and larger rapidity regions, contribution from intrinsic charm are more obvious.

D. Theoretical uncertainties for Ξ_{cc} production

In this subsection, we discuss the main theoretical uncertainties for the Ξ_{cc} production at the After@LHC, which are from the choices of the charm quark mass, the renormalization scale, and the intrinsic charm PDF, respectively. When discussing the uncertainty from one error source, other input parameters shall be kept to be their central values. For convenience, we set $A_{\text{in}} = 1\%$ throughout this subsection.

m_c (GeV)	1.65	1.75	1.85
$g + g \rightarrow (cc)_{\bar{3}}[{}^3S_1]$	1.27×10^3	7.55×10^2	4.57×10^2
$g + g \rightarrow (cc)_{\bar{6}}[{}^1S_0]$	2.32×10^2	1.37×10^2	8.24×10^1
$g + c \rightarrow (cc)_{\bar{3}}[{}^3S_1]$	7.58×10^3	5.32×10^3	3.76×10^3
$g + c \rightarrow (cc)_{\bar{6}}[{}^1S_0]$	8.22×10^2	5.78×10^2	4.09×10^2
$c + c \rightarrow (cc)_{\bar{3}}[{}^3S_1]$	3.24	1.79	1.25
$c + c \rightarrow (cc)_{\bar{6}}[{}^1S_0]$	1.33×10^{-1}	7.16×10^{-2}	5.12×10^{-2}

TABLE IX. Total cross sections (in unit pb) for the Ξ_{cc} production at the After@LHC under different choices of m_c mass. $p_t > 0.2$ GeV and $A_{\text{in}} = 1\%$.

Total cross sections for $m_c = 1.75 \pm 0.10$ GeV are presented in Table IX, which shows

$$\begin{aligned} \sigma_{g+g \rightarrow (cc)_{\bar{3}}[{}^3S_1]} &= (7.55^{+5.15}_{-2.98}) \times 10^2 \text{ pb}, \\ \sigma_{g+g \rightarrow (cc)_{\bar{6}}[{}^1S_0]} &= (1.37^{+0.95}_{-0.55}) \times 10^2 \text{ pb}, \\ \sigma_{g+c \rightarrow (cc)_{\bar{3}}[{}^3S_1]} &= (5.69^{+2.44}_{-1.68}) \times 10^3 \text{ pb}, \\ \sigma_{g+c \rightarrow (cc)_{\bar{6}}[{}^1S_0]} &= (6.19^{+2.64}_{-1.82}) \times 10^2 \text{ pb}, \\ \sigma_{c+c \rightarrow (cc)_{\bar{3}}[{}^3S_1]} &= 2.02^{+1.61}_{-0.59} \text{ pb}, \\ \sigma_{c+c \rightarrow (cc)_{\bar{6}}[{}^1S_0]} &= (8.03^{+6.77}_{-2.25}) \times 10^{-2} \text{ pb}. \end{aligned} \quad (15)$$

Total cross section depends heavily on the choice of charm quark mass, which shall be changed by $[-39\%, 69\%]$ for $g + g$ channel, $[-30\%, 43\%]$ for $g + c$ channel, and $[-29\%, 84\%]$ for the $c + c$ channel, respectively.

μ_R	$\sqrt{\hat{s}}$	$\sqrt{\hat{s}}/2$	M_t
$g + g \rightarrow (cc)_{\bar{3}}[{}^3S_1]$	1.63×10^2	3.99×10^2	7.55×10^2
$g + g \rightarrow (cc)_{\bar{6}}[{}^1S_0]$	3.13×10^1	7.67×10^1	1.37×10^2
$g + c \rightarrow (cc)_{\bar{3}}[{}^3S_1]$	3.43×10^3	5.47×10^3	5.32×10^3
$g + c \rightarrow (cc)_{\bar{6}}[{}^1S_0]$	3.76×10^2	5.99×10^2	5.78×10^2
$c + c \rightarrow (cc)_{\bar{3}}[{}^3S_1]$	1.25	1.76	1.79
$c + c \rightarrow (cc)_{\bar{6}}[{}^1S_0]$	5.05×10^{-2}	7.03×10^{-2}	7.16×10^{-2}

TABLE X. Total cross sections (in unit pb) for the Ξ_{cc} production at the After@LHC under different choices of renormalization scale μ_R . $p_t > 0.2$ GeV and $A_{\text{in}} = 1\%$.

In the above estimations, we have fixed the renormalization scale μ_R to be the transverse mass of Ξ_{cc} , e.g., $m_T = \sqrt{p_t^2 + M_{\Xi_{cc}}^2}$, which is usually adopted in the literature. Taking another two choices, e.g., $\mu_R = \sqrt{\hat{s}}/2$ and $\mu_R = \sqrt{\hat{s}}$, we estimate the renormalization scale uncertainty, where $\sqrt{\hat{s}}$ is the center-of-mass energy of the subprocess. Numerical results are presented in Table X. For the case of Ξ_{cc} production via $(g + c)$ channel, the scale uncertainty is about $\pm 35\%$.

	σ_{g+c} (pb)		σ_{c+c} (pb)	
	$(cc)_{\bar{3}}[{}^3S_1]$	$(cc)_{\bar{6}}[{}^1S_0]$	$(cc)_{\bar{3}}[{}^3S_1]$	$(cc)_{\bar{6}}[{}^1S_0]$
BHPS	5.32×10^3	5.78×10^2	1.79	7.16×10^{-2}
CT14C-BHPS1	6.39×10^3	6.95×10^2	1.68	6.77×10^{-2}
CT14C-SEA1	6.79×10^3	7.39×10^2	1.26	5.15×10^{-2}

TABLE XI. Total cross sections for three different intrinsic charm PDFs. CT14+BHPS is result by using the BHPS model evolved with Eq.(5), CT14C-BHPS1 and CT14C-SEA1 are results for the CTEQ PDFs under BHPS model and SEA model [65], respectively. All the intrinsic charm PDFs are normalized to 1%. $p_t > 0.2$ GeV.

To show how different models of IC PDF affect the production rates, we adopt the CTEQ PDF version CT14C under BHPS model, SEA model [65] as explicit examples to estimate the errors caused by different choices of the IC PDF. The results are shown in Table XI. Both the CT14C-BHPS1 and CT14C-SEA1 are characterized by the magnitude of the intrinsic charm component by the first moment of the charm distribution $\langle x \rangle_{\text{IC}} = 0.57\%$, which corresponds to 1% probability for finding intrinsic charm component in a proton. Table XI shows that by using those three IC PDFs, the total cross sections vary by about 20% \sim 27% and 6% \sim 30% for the $(g + c)$ and $(c + c)$ mechanisms, respectively.

As a final remark, if choosing the recently developed model independent NNPDF3IC [64] as the input for the IC PDF, whose input parameters are based on a NLO calculation and are fixed via a global fitting of experimental data of deep inelastic structure functions, we

	σ_{g+c} (pb)		σ_{c+c} (pb)	
	$(cc)_{\mathbf{3}}[{}^3S_1]$	$(cc)_{\mathbf{6}}[{}^1S_0]$	$(cc)_{\mathbf{3}}[{}^3S_1]$	$(cc)_{\mathbf{6}}[{}^1S_0]$
NNPDF3IC-1330	4.85×10^3	5.27×10^2	1.49	5.97×10^{-2}
NNPDF3IC-1610	4.49×10^3	4.86×10^2	1.45	5.78×10^{-2}
CT10C-BHPS1	5.99×10^3	6.51×10^2	1.50	6.03×10^{-2}
CT10C-SEA1	6.33×10^3	6.88×10^2	1.14	4.67×10^{-2}

TABLE XII. Total cross sections for different choices of intrinsic charm PDF with various IC models. $p_t > 0.2$ GeV.

shall obtain a slightly smaller total cross-sections than the cases of CT14+BHPS and CT14C-BHPS1². The NNPDF3IC results are presented in Tab. XII, which are for the NNPDF3IC preferable m_c range of [1.33, 1.61] GeV.

IV. CONCLUSIONS

In the paper, we have studied the hadronic production of Ξ_{cc} baryon at the fixed-target experiment at the LHC, e.g. After@LHC. More accurate data are assumed to be available at the After@LHC than the SELEX experiment, which shall be helpful to clarify the previous SELEX puzzle on the Ξ_{cc} production. Our results show that the intrinsic charm can have significant impact on the Ξ_{cc} production. If setting the probability of finding the intrinsic charm in proton is $A_{in} = 1\%$, the total production cross section can be enhanced by a factor of 2 through the

$(g+c)$ and $(c+c)$ channels. By summing up contributions from $(g+g)$, $(g+c)$, and $(c+c)$ channels and contributions from both diquark states $(cc)_{\mathbf{3}}[{}^3S_1]$ and $(cc)_{\mathbf{6}}[{}^1S_0]$, we shall have 3.4×10^5 or 1.4×10^7 Ξ_{cc} events per operation year with the integrated luminosity 0.05 fb^{-1} or 2 fb^{-1} , respectively.

Thus, the fixed-target experiment After@LHC can be an ideal platform for studying properties of Ξ_{cc} . Since the total cross sections and the differential distributions are sensitive to the probability of finding intrinsic charm component in a proton, the After@LHC shall also be a good platform for testing the intrinsic charm mechanism and for fixing the intrinsic charm PDF.

Acknowledgements: We thank Hua-Yong Han and Yun-Qing Tang for helpful discussions on the intrinsic charm PDF. This work was supported in part by the Natural Science Foundation of China under Grant No.11605029, No.11625520, and No.11847301, and by the Fundamental Research Funds for the Central Universities under Grant No.2019CDJDWL0005.

-
- [1] R. Aaij *et al.* [LHCb Collaboration], “Observation of the doubly charmed baryon Ξ_{cc}^{++} ,” *Phys. Rev. Lett.* **119**, 112001 (2017).
- [2] R. Aaij *et al.* [LHCb Collaboration], “Physics case for an LHCb Upgrade II - Opportunities in flavour physics, and beyond, in the HL-LHC era,” arXiv:1808.08865.
- [3] A. F. Falk, M. E. Luke, M. J. Savage, and M. B. Wise, “Heavy quark fragmentation to baryons containing two heavy quarks,” *Phys. Rev. D* **49**, 555 (1994).
- [4] V. V. Kiselev, A. K. Likhoded, and M. V. Shevlyagin, “Double charmed baryon production at B factory,” *Phys. Lett. B* **332**, 411 (1994).
- [5] S. P. Baranov, “On the production of doubly flavored baryons in pp , ep , and $\gamma\gamma$ collisions,” *Phys. Rev. D* **54**, 3228 (1996).
- [6] A. V. Berezhnoy, V. V. Kiselev, A. K. Likhoded, and A. I. Onishchenko, “Doubly charmed baryon production in hadronic experiments,” *Phys. Rev. D* **57**, 4385 (1998).
- [7] D. A. Gunter and V. A. Saleev, “Hadronic production of doubly charmed baryons via charm excitation in proton,” *Phys. Rev. D* **64**, 034006 (2001).
- [8] V. V. Braguta, V. V. Kiselev, and A. E. Chalov, “Pair production of doubly heavy diquarks,” *Phys. Atom. Nucl.* **65**, 1537 (2002).
- [9] J. P. Ma and Z. G. Si, “Factorization approach for inclusive production of doubly heavy baryon,” *Phys. Lett. B* **568**, 135 (2003).
- [10] E. Braaten, M. Kusunoki, Y. Jia, and T. Mehen, “ Λ_c^+/Λ_c^- asymmetry in hadroproduction from heavy quark recombination,” *Phys. Rev. D* **70**, 054021 (2004).
- [11] S. Y. Li, Z. G. Si, and Z. J. Yang, “Doubly heavy baryon production at gamma gamma collider,” *Phys. Lett. B* **648**, 284 (2007).
- [12] Z. J. Yang and T. Yao, “Doubly heavy baryon production at polarized photon collider,” *Chin. Phys. Lett.* **24**, 3378
-
- ² A smaller total cross-section is reasonable, since the fitted NNPDF3IC prefers a scale-dependent probability of finding IC component in a proton, e.g. $0.7\% \pm 0.3\%$ for the scale equals to 1.65 GeV [64], which is smaller than our present choice of 1% for CT14+BHPS and CT14C-BHPS1; More over, the NNPDF3IC PDF becomes negative for $x \gtrsim 0.75$.

- (2007).
- [13] J. W. Zhang, X. G. Wu, T. Zhong, Y. Yu, and Z. Y. Fang, “Hadronic production of the doubly heavy baryon Ξ_{bc} at LHC,” *Phys. Rev. D* **83**, 034026 (2011).
- [14] J. Jiang, X. G. Wu, Q. L. Liao, X. C. Zheng, and Z. Y. Fang, “Doubly heavy baryon production at a high luminosity e^+e^- collider,” *Phys. Rev. D* **86**, 054021 (2012).
- [15] J. Jiang, X. G. Wu, S. M. Wang, J. W. Zhang, and Z. Y. Fang, “A further study on the doubly heavy baryon production around the Z^0 peak at a high luminosity e^+e^- collider,” *Phys. Rev. D* **87**, 054027 (2013).
- [16] A. P. Martynenko and A. M. Trunin, “Relativistic corrections to the pair double heavy diquark production in $e^+e^- \rightarrow$ annihilation,” *Phys. Rev. D* **89**, 014004 (2014).
- [17] G. Chen, X. G. Wu, Z. Sun, Y. Ma, and H. B. Fu, “Photoproduction of doubly heavy baryon at the ILC,” *J. High Energy Phys.* **12** (2014) 018.
- [18] Z. J. Yang and X. X. Zhao, “The production of Ξ_{bb} at photon collider,” *Chin. Phys. Lett.* **31**, 091301 (2014).
- [19] Z. J. Yang, P. F. Zhang, and Y. J. Zheng, “Doubly heavy baryon production in e^+e^- annihilation,” *Chin. Phys. Lett.* **31**, 051301 (2014).
- [20] A. P. Martynenko and A. M. Trunin, “Pair double heavy diquark production in high energy proton-proton collisions,” *Eur. Phys. J. C* **75**, 138 (2015).
- [21] W. K. Lai and A. K. Leibovich, “ Λ_c^+/Λ_c^- and $\Lambda_b^0/\bar{\Lambda}_b^0$ production asymmetry at the LHC from heavy quark recombination,” *Phys. Rev. D* **91**, 054022 (2015).
- [22] Z. S. Brown, W. Detmold, S. Meinel, and K. Orginos, “Charmed bottom baryon spectroscopy from lattice QCD,” *Phys. Rev. D* **90**, 094507 (2014).
- [23] X. C. Zheng, C. H. Chang and Z. Pan, “Production of doubly heavy-flavored hadrons at e^+e^- colliders,” *Phys. Rev. D* **93**, 034019 (2016).
- [24] A. Trunin, “bc diquark pair production in high energy proton-proton collisions,” *Phys. Rev. D* **93**, 114029 (2016).
- [25] A. V. Berezhnoy and A. K. Likhoded, “Doubly heavy baryons,” *Phys. Atom. Nucl.* **79**, 260 (2016).
- [26] S. J. Brodsky, S. Groote and S. Koshkarev, “Resolving the SELEX-LHCb double-charm baryon conflict: the impact of intrinsic heavy-quark hadroproduction and supersymmetric light-front holographic QCD,” *Eur. Phys. J. C* **78**, 483 (2018).
- [27] H. Y. Bi, R. Y. Zhang, X. G. Wu, W. G. Ma, X. Z. Li, and S. Owusu, “Photoproduction of doubly heavy baryon at the LHeC,” *Phys. Rev. D* **95**, 074020 (2017).
- [28] X. Yao and B. Muller, “Doubly charmed baryon production in heavy ion collisions,” *Phys. Rev. D* **97**, 074003 (2018).
- [29] J. J. Niu, L. Guo, H. H. Ma, X. G. Wu, and X. C. Zheng, “Production of semi-inclusive doubly heavy baryons via top-quark decays,” *Phys. Rev. D* **98**, 094021 (2018).
- [30] V. N. Gribov and L. N. Lipatov, “Deep inelastic e p scattering in perturbation theory,” *Sov. J. Nucl. Phys.* **15**, 438 (1972).
- [31] G. Altarelli and G. Parisi, “Asymptotic freedom in parton language,” *Nucl. Phys.* **B126**, 298 (1977).
- [32] Y. L. Dokshitzer, “Calculation of the structure functions for deep Inelastic scattering and e^+e^- annihilation by perturbation theory in quantum chromodynamics,” *Sov. Phys. JETP* **46**, 641 (1977).
- [33] C. H. Chang, C. F. Qiao, J. X. Wang, and X. G. Wu, “Estimate of the hadronic production of the doubly charmed baryon Ξ_{cc} under GM-VFN scheme,” *Phys. Rev. D* **73**, 094022 (2006).
- [34] G. Chen, X. G. Wu, J. W. Zhang, H. Y. Han, and H. B. Fu, “Hadronic production of Ξ_{cc} at a fixed-target experiment at the LHC,” *Phys. Rev. D* **89**, 074020 (2014).
- [35] G. Chen, C. H. Chang, and X. G. Wu, “Hadronic production of the doubly charmed baryon via the protonnucleus and the nucleusnucleus collisions at the RHIC and LHC,” *Eur. Phys. J. C* **78**, 801 (2018).
- [36] S. J. Brodsky, F. Fleuret, C. Hadjidakis and J. P. Lansberg, “Physics opportunities of a fixed-target experiment using the LHC Beams,” *Phys. Rept.* **522**, 239 (2013).
- [37] C. Hadjidakis *et al.*, “A Fixed-Target Programme at the LHC: physics case and projected performances for heavy-Ion, hadron, spin and astroparticle studies,” arXiv:1807.00603 [hep-ex].
- [38] J. P. Lansberg *et al.*, “A Fixed-Target Experiment at the LHC (AFTER@LHC) : luminosities, target polarisation and a selection of physics studies,” *PoS QNP* **2012**, 049 (2012).
- [39] J. P. Lansberg *et al.*, “Prospects for A Fixed-Target Experiment at the LHC: AFTER@LHC,” *PoS ICHEP* **2012**, 547 (2013).
- [40] J. P. Lansberg *et al.*, “AFTER@LHC: a precision machine to study the interface between particle and nuclear physics,” *EPJ Web Conf.* **66** (2014) 11023.
- [41] S. J. Brodsky, P. Hoyer, C. Peterson, and N. Sakai, “The intrinsic charm of the proton,” *Phys. Lett.* **93B**, 451 (1980).
- [42] S. J. Brodsky, C. Peterson, and N. Sakai, “Intrinsic heavy quark states,” *Phys. Rev. D* **23**, 2745 (1981).
- [43] S. J. Brodsky, A. Kusina, F. Lyonnet, I. Schienbein, H. Spiesberger, and R. Vogt, “A review of the intrinsic heavy quark content of the nucleon,” *Adv. High Energy Phys.* **2015**, 231547 (2015).
- [44] F. S. Navarra, M. Nielsen, C. A. A. Nunes, and M. Teixeira, “On the intrinsic charm component of the nucleon,” *Phys. Rev. D* **54**, 842 (1996).
- [45] T. J. Hobbs, J. T. Londergan, and W. Melnitchouk, “Phenomenology of nonperturbative charm in the nucleon,” *Phys. Rev. D* **89**, 074008 (2014).
- [46] J. Pumplin, “Light-cone models for intrinsic charm and bottom,” *Phys. Rev. D* **73**, 114015 (2006).
- [47] C. H. Chang, J. P. Ma, C. F. Qiao, and X. G. Wu, “Hadronic production of the doubly charmed baryon Ξ_{cc} with intrinsic charm,” *J. Phys. G* **34**, 845 (2007).
- [48] S. Koshkarev and V. Anikeev, “Production of the doubly charmed baryons at the SELEX experiment-The double intrinsic charm approach,” *Phys. Lett. B* **765**, 171 (2017).
- [49] S. Koshkarev, “Production of the doubly heavy baryons, B_c meson and the all-charm tetraquark at AFTER@LHC with double intrinsic heavy mechanism,” *Acta Phys. Polon. B* **48**, 163 (2017).
- [50] S. Groote and S. Koshkarev, “Production of doubly charmed baryons nearly at rest,” *Eur. Phys. J. C* **77**, 509 (2017).
- [51] M. Mattson *et al.* [SELEX Collaboration], “First Observation of the Doubly Charmed Baryon Ξ_{cc}^+ ,” *Phys. Rev. Lett.* **89**, 112001 (2002).
- [52] A. Ocherashvili *et al.* [SELEX Collaboration], “Confirmation of the double charm baryon $\Xi^+(cc)(3520)$ via

- its decay to $p D^+ K^-$,” *Phys. Lett. B* **628**, 18 (2005).
- [53] M. A. G. Aivazis, F. I. Olness, and W. K. Tung, “Leptoproduction of heavy quarks. 1. General formalism and kinematics of charged current and neutral current production processes,” *Phys. Rev. D* **50**, 3085 (1994).
- [54] M. A. G. Aivazis, J. C. Collins, F. I. Olness, and W. K. Tung, “Leptoproduction of heavy quarks. 2. A Unified QCD formulation of charged and neutral current processes from fixed target to collider energies,” *Phys. Rev. D* **50**, 3102 (1994).
- [55] F. I. Olness, R. J. Scalise, and W. K. Tung, “Heavy quark hadroproduction in perturbative QCD,” *Phys. Rev. D* **59**, 014506 (1999).
- [56] J. Amundson, C. Schmidt, W. K. Tung, and X. Wang, “Charm production in deep inelastic scattering from threshold to high Q^2 ,” *J. High Energy Phys.* **10** (2000) 031.
- [57] R. D. Field, “Applications of perturbative QCD,” *Front. Phys.* **77**, 1 (1989).
- [58] J. Pumplin, H. L. Lai, and W. K. Tung, “The Charm Parton Content of the Nucleon,” *Phys. Rev. D* **75**, 054029 (2007).
- [59] P. M. Nadolsky, H. L. Lai, Q. H. Cao, J. Huston, J. Pumplin, D. Stump, W. K. Tung, and C.-P. Yuan, “Implications of CTEQ global analysis for collider observables,” *Phys. Rev. D* **78**, 013004 (2008).
- [60] A. D. Martin, W. J. Stirling, R. S. Thorne, and G. Watt, “Parton distributions for the LHC,” *Eur. Phys. J. C* **63**, 189 (2009).
- [61] S. Dulat, T. J. Hou, J. Gao, J. Huston, J. Pumplin, C. Schmidt, D. Stump, and C. P. Yuan, “Intrinsic Charm Parton Distribution Functions from CTEQ-TEA Global Analysis,” *Phys. Rev. D* **89**, 073004 (2014).
- [62] P. Jimenez-Delgado, T. J. Hobbs, J. T. Londergan, and W. Melnitchouk, “New limits on intrinsic charm in the nucleon from global analysis of parton distributions,” *Phys. Rev. Lett.* **114**, 082002 (2015).
- [63] F. Lyonnet, A. Kusina, T. Jeo, K. Kovark, F. Olness, I. Schienbein, and J. Y. Yu, “On the intrinsic bottom content of the nucleon and its impact on heavy new physics at the LHC,” *JHEP* **1507**, 141 (2015).
- [64] R. D. Ball *et al.* [NNPDF Collaboration], “A Determination of the Charm Content of the Proton,” *Eur. Phys. J. C* **76**, 647 (2016).
- [65] T. J. Hou *et al.*, “CT14 Intrinsic Charm Parton Distribution Functions from CTEQ-TEA Global Analysis,” *JHEP* **1802**, 059 (2018).
- [66] The CT14 LO PDF is issued by the CTEQ group and can be downloaded from the webpage, <https://hep.pa.msu.edu/cteq/public/index.html>.
- [67] C. H. Chang, J. X. Wang, and X. G. Wu, “GENXICC: A generator for hadronic production of the double heavy baryons Ξ_{cc} , Ξ_{bc} and Ξ_{bb} ,” *Comput. Phys. Commun.* **177**, 467 (2007).
- [68] C. H. Chang, J. X. Wang, and X. G. Wu, “GENXICC2.0: An upgraded version of the generator for hadronic production of double heavy baryons Ξ_{cc} , Ξ_{bc} and Ξ_{bb} ,” *Comput. Phys. Commun.* **181**, 1144 (2010).
- [69] X. Y. Wang and X. G. Wu, “GENXICC2.1: An improved version of GENXICC for hadronic production of doubly heavy baryons,” *Comput. Phys. Commun.* **184**, 1070 (2013).